Characterizing the dayside auroral ionosphere with ISR elevation scans and field-aligned observations

Ingeborg Frøystein[1], Andres Spicher[1], Kjellmar Oksavik[2,3], Björn Gustavsson[1], and Magnar Gullikstad Johnsen[4]

[1]Department of Physics and Technology, UiT The Arctic University of Norway, Tromsø, Norway, [2]Department of Physics and Technology, University of Bergen, Bergen, Norway
[3]Department of Arctic Geophysics, The University Centre in Svalbard, Longyearbyen, Norway, [4]Tromsø Geophysical Observatory, Tromsø, Norway

✉ Contact: Ingeborg.froystein@uit.no

This presentation participates in OSPP
Outstanding Student & PhD candidate Presentation contest

1. Introduction and overview

- The dayside auroral region is a dynamic and unique part of the ionosphere due to its coupling to the solar wind-magnetosphere system → extensively studied by a myriad of instruments, both ground-based (e.g. Milan et al., Nilsson et al., Lockwood et al., Johnsen et al.) and in-situ (e.g. Newell et al.)
- Incoherent Scatter Radars (ISR) provide observations on the ionospheric parameters T_e, T_i and N_e across altitudes in the radar pointing direction. Varying the radar elevation ("scanning") also gives the ionospheric parameters across a latitude range.

In this study: using EISCAT Svalbard radar (ESR) elevation scans and field-aligned observations, we determine the latitude of the open-closed field line boundary (OCB) and separate the ionosphere into three regions: (1) closed field lines, (2) along the OCB, and (3) polar cap. Together, the observations on open and closed field lines from both elevation scans and field aligned measurements contribute to a characterization of the dayside auroral ionosphere.

2. Data set

In this study, scans from the ESR 32 meter and field-aligned observations from the ESR 42 meter are used.

- 32 meter: ~100 hours, 2002-2015
- 42 meter: ~ 1300 hours, 2001-2023

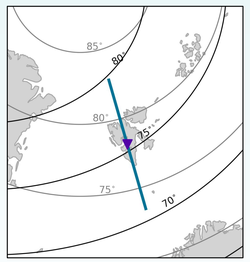


Figure 1↑: Map of Svalbard with the ESR 32 m FOV and 42 m position.

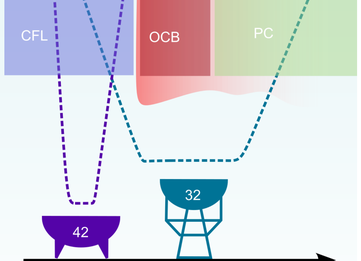


Figure 2↑: Schematic of the identified regions based on the T_e and N_e ISR method, showing the ESR 32 m FOV, 42 m FOV, the polar cap, along the OCB and closed field lines.

3.1 Method – identify the OCB

Low energy dayside auroral precipitation leads to electron heating at high altitudes. The dayside auroral region is therefore defined as where T_e is enhanced above a set threshold

$$T_e\ (300\ km) > T_{e,threshold}(N_e)$$

$T_{e,threshold}(N_e)$ is an adaptive threshold, which is adjusted to account for variation in the background N_e. The equatorward edge of the enhanced T_e region is the OCB. From the OCB and 3 degrees poleward is classified as along the OCB. Poleward is the PC, and equatorward is CFL.

The method and threshold $T_{e,threshold}(N_e)$ is described in detail in:
Frøystein, I., Spicher, A., Gustavsson, B., Oksavik, K., & Johnsen, M. G. (2024). On the identification of the dayside auroral region using incoherent scatter radar. Journal of Geophysical Research: Space Physics, 129, e2024JA033361. https://doi.org/10.1029/2024JA033361

Acknowledgements
The EISCAT data is obtained from the EISCAT Portal and the EISCAT Madrigal database. EISCAT is an international association supported by research organizations in China (CRIRP), Finland (SA), Japan (NIPR and ISEE), Norway (NFR), Sweden (VR), and the United Kingdom (UKRI). The IMF data is retrieved through the OMNIWeb. The sunspot numbers are retrieved from WDC-SILSO, Royal Observatory of Belgium, Brussels, DOI: https://doi.org/10.24414/qnza-ac80. AS acknowledges funding from NRC (Grant 32603) during part of the project. Figures 3, 6, 7 and 8 are adapted from Frøystein et al. (2025; preprint under review; ANGEO).

3.2 Method - identified CFL, OCB and PC

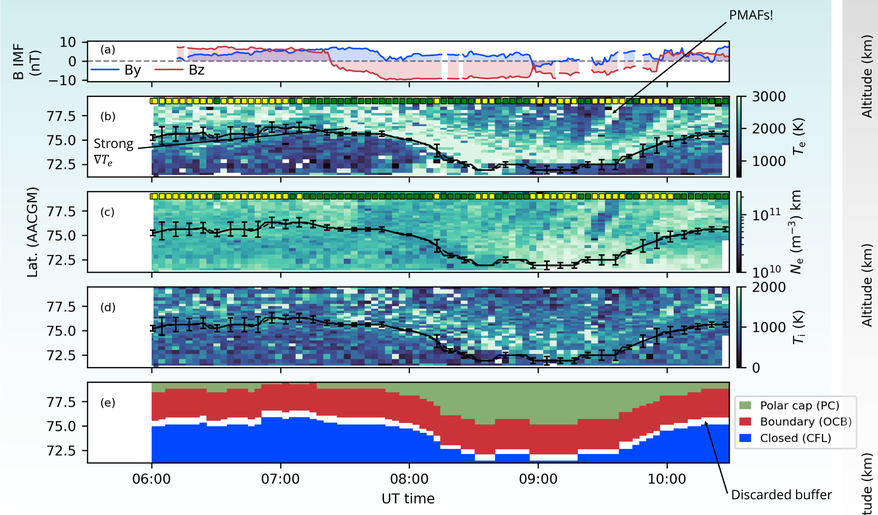
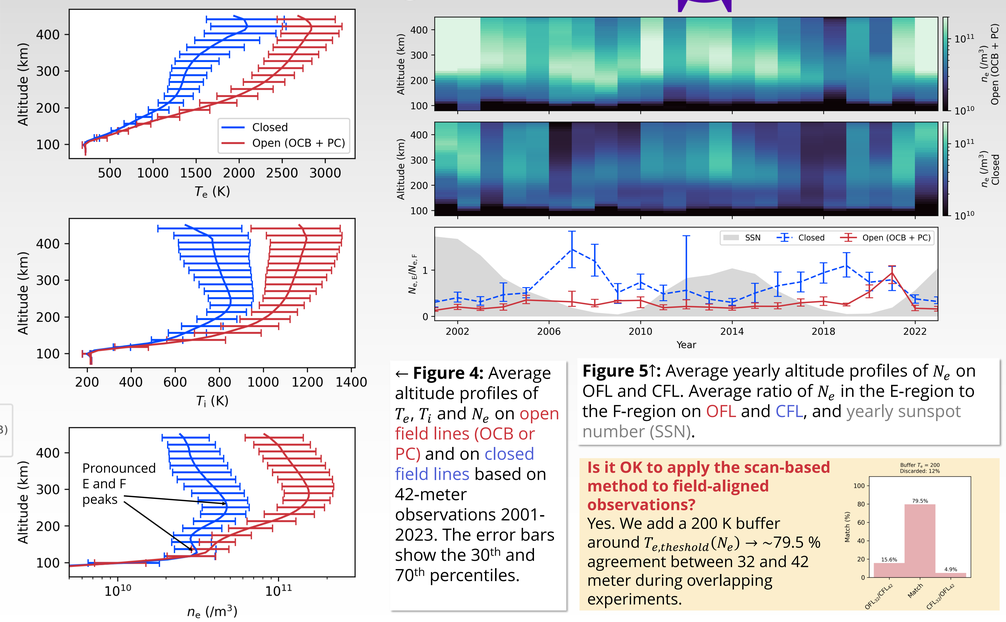


Figure 3↑: Example experiment showing IMF B_z and B_y, T_e, N_e, T_i, the identified OCB, and the extracted regions on CFL, along the OCB and in the PC. The colored squares are OCB latitude quality flags.

4.1 Statistical results: field-aligned observations

42



← **Figure 4:** Average altitude profiles of T_e, T_i and N_e on open field lines (OCB or PC) and on closed field lines based on 42-meter observations 2001-2023. The error bars show the 30th and 70th percentiles.

Figure 5↑: Average yearly altitude profiles of N_e on OFL and CFL. Average ratio of N_e in the E-region to the F-region on OFL and CFL, and yearly sunspot number (SSN).

Is it OK to apply the scan-based method to field-aligned observations?
Yes. We add a 200 K buffer around $T_{e,theshold}(N_e)$ → ~79.5 % agreement between 32 and 42 meter during overlapping experiments.

4.2 Statistical results: elevation scans

32

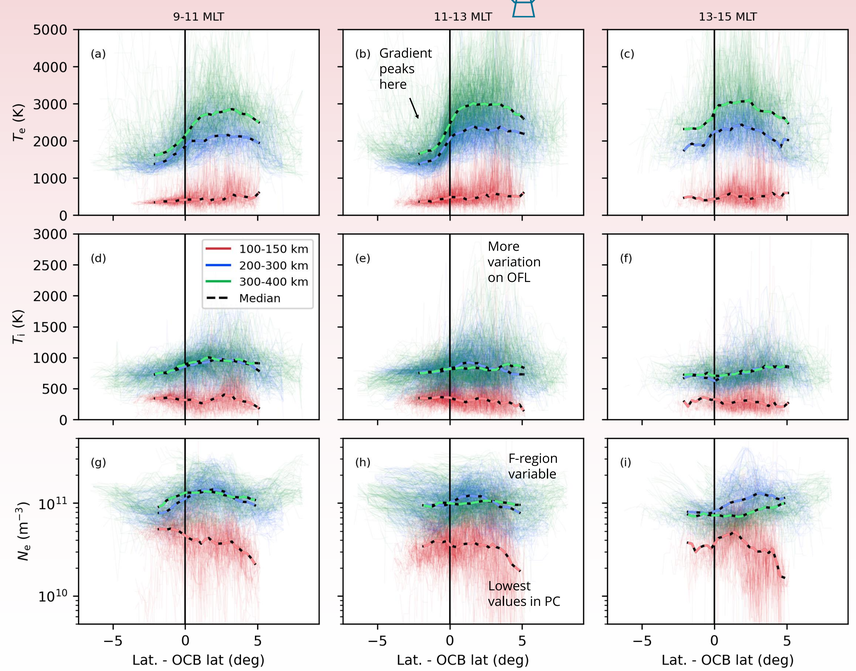


Figure 6↑: Ionospheric T_e, T_i and N_e as a function of distance from the OCB at 100-150, 200-300 and 300-400 km altitude.

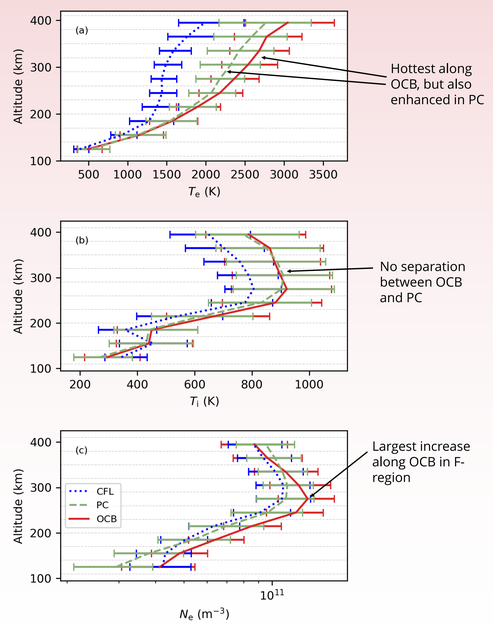


Figure 7↑: Average altitude profiles of T_e, T_i and N_e in the polar cap, along the OCB and on closed field lines. The error bars show the 30th and 70th percentiles per 30 km altitude.

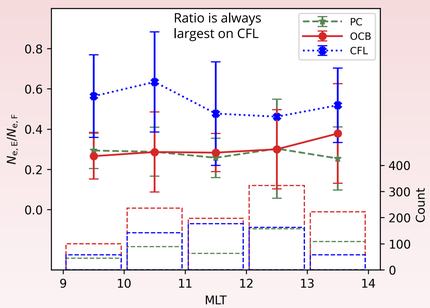


Figure 8↑: Average ratio between N_e in the E and F regions in the polar cap, along the OCB and on closed field lines.

5. Outlook/future work

- What about the ion velocity v_i?
- Solar cycle variation within and outside the auroral region?
- What about azimuthal radar scans?
- Derived parameters, e.g. ionospheric conductivities?

References
Burrell, A. G., van der Meeren, C., Laundal, K. M., & van Kemenade, H. (2023, February). aburrell/aacgmv2: Version 2.6.3. Zenodo. doi: 10.5281/zenodo.7621545 • Frøystein, I., Spicher, A., Gustavsson, B., Oksavik, K., & Johnsen, M. G. (2024). On the identification of the dayside auroral region using incoherent scatter radar. Journal of Geophysical Research: Space Physics, 129, e2024JA033361. https://doi.org/10.1029/2024JA033361 • Johnsen, M. G., Lorentzen, D. A., Holmes, J. M., & Lanhuag, U. P. (2012, March). A model-based method for obtaining the open/closed field line boundary from the cusp auroral 630.0 [OI] red line. Journal of Geophysical Research (Space Physics), 117 (A3), A03319. doi: 10.1029/2011JA016980 • Lockwood, M., Moen, J., van Eyken, A. P., Davies, J. A., Oksavik, K., and McCrea, I. W.: Motion of the dayside polar cap boundary during substorm cycles: I. Observations of pulses in the magnetopause reconnection rate, Ann. Geophys., 23, 3495–3511, https://doi.org/10.5194/angeo-23-3495-2005, 2005. • Milan, S. E., Lester, M., Cowley, S. W. H., Moen, J., Sandholt, P. E., & Owen, C. J. (1999). Meridian-scanning photometer, coherent HF radar, and magnetometer observations of the cusp: a case study. Annales Geophysicae, 17 (2), 159–172. doi: 10.1007/s00585-999-0159-5 • Newell, P. T., Ruohoniemi, J. M., & Meng, C. I. (2004, October). Maps of precipitation by source region, binned by IMF, with inertial convection streamlines. Journal of Geophysical Research (Space Physics), 109 (A10), A10206. doi: 10.1029/2004JA010499 • Nilsson, H., Yamauchi, M., Eliasson, L., Norberg, O., & Clemmons, J. (1996, May). Ionospheric signature of the cusp as seen by incoherent scatter radar. Journal of Geophysical Research (Space Physics), 101 (A5), 10947–10964. doi: 10.1029/95JA03341 • Papitashvili, Natalia E. and King, Joseph H. (2020), "OMNI 1-min Data" [data set], NASA Space Physics Data Facility, https://doi.org/10.48322/45bb-8792, Accessed on 23.11.26.